Noise immune cavity enhanced optical heterodyne velocity modulation spectroscopy

Brian M. Siller,[1] Michael W. Porambo,[1] Andrew A. Mills[1] and Benjamin J. McCall[1,2,*]

[1]*Department of Chemistry, University of Illinois at Urbana-Champaign, Urbana, IL, 61801*
[2]*Departments of Astronomy and Physics, University of Illinois at Urbana-Champaign, Urbana, IL, 61801*
[*]*bjmccall@illinois.edu*

http://bjm.scs.illinois.edu/

Abstract: The novel technique of cavity enhanced velocity modulation spectroscopy has recently been demonstrated as the first general absorption technique that allows for sub-Doppler spectroscopy of molecular ions while retaining ion-neutral discrimination. The previous experimental setup has been further improved with the addition of heterodyne detection in a NICE-OHMS setup. This improves the sensitivity by a factor of 50 while retaining sub-Doppler resolution and ion-neutral discrimination. Calibration was done with an optical frequency comb, and line centers for several N_2^+ lines have been determined to within an accuracy of 300 kHz.

OCIS codes: (300.1030) Absorption; (300.6320) Spectroscopy, high-resolution; (300.6460) Spectroscopy, saturation; (300.6380) Spectroscopy, modulation; (300.6390) Spectroscopy, molecular; (300.6340) Spectroscopy, infrared.

References and links

1. S. K. Stephenson and R. J. Saykally, "Velocity modulation spectroscopy of ions," Chem. Rev. **105**, 3220–3234 (2005).
2. B. M. Siller, A. A. Mills, and B. J. McCall, "Cavity-enhanced velocity modulation spectroscopy," Opt. Lett. **35**, 1266–1268 (2010).
3. A. A. Mills, B. M. Siller, and B. J. McCall, "Precision cavity enhanced velocity modulation spectroscopy," Chem. Phys. Lett. **501**, 1 – 5 (2010).
4. J. Ye, L. S. Ma, and J. L. Hall, "Ultrasensitive detections in atomic and molecular physics: demonstration in molecular overtone spectroscopy," J. Opt. Soc. Am. B **15**, 6–15 (1998).
5. A. Foltynowicz, F. M. Schmidt, W. Ma, and O. Axner, "Noise-immune cavity-enhanced optical heterodyne molecular spectroscopy: Current status and future potential," Appl. Phys. B **92**, 313–326 (2008).
6. R. D. L. Kronig, "On the theory of dispersion of x-rays," J. Opt. Soc. Am. **12**, 547–556 (1926).
7. A. Foltynowicz, W. Ma, F. M. Schmidt, and O. Axner, "Wavelength-modulated noise-immune cavity-enhanced optical heterodyne molecular spectroscopy signal line shapes in the Doppler limit," J. Opt. Soc. Am. B **26**, 1384–1394 (2009).
8. E. A. Donley, T. P. Heavner, F. Levi, M. O. Tataw, and S. R. Jefferts, "Double-pass acousto-optic modulator system," Rev. Sci. Instrum. **76**, 063112 (2005).
9. R. W. P. Drever, J. L. Hall, F. V. Kowalski, J. Hough, G. M. Ford, A. J. Munley, and H. Ward, "Laser phase and frequency stabilization using an optical-resonator," Appl. Phys. B **31**, 97–105 (1983).
10. W. Ma, A. Foltynowicz, and O. Axner, "Theoretical description of doppler-broadened noise-immune cavity-enhanced optical heterodyne molecular spectroscopy under optically saturated conditions," J. Opt. Soc. Am. B **25**, 1144–1155 (2008).

#151471 - $15.00 USD Received 28 Jul 2011; revised 10 Oct 2011; accepted 17 Oct 2011; published 18 Nov 2011

11. M. S. Child, *Molecular Collision Theory* (Academic Press Inc, 1974).
12. R. G. DeVoe and R. G. Brewer, "Laser-frequency division and stabilization," Phys. Rev. A. **30**, 2827–2829 (1984).

1. Introduction

1.1. Velocity modulation spectroscopy

Laboratory spectroscopy of molecular ions is of great interest to a variety of fields, but is typically difficult because even in laboratory plasmas designed to observe a particular ion, the ion of interest has a very low concentration, typically orders of magnitude lower than that of any ambient neutral molecules in discharge cells. Velocity Modulation Spectroscopy (VMS) in positive column discharge cells has been the most commonly used technique in this field over the past few decades because it combines the advantages of relatively high ion density and ion-neutral discrimination [1].

Recently, a new method of performing VMS has been demonstrated by placing the plasma discharge cell within an optical cavity in a technique we call Cavity Enhanced Velocity Modulation Spectroscopy (CEVMS) [2, 3]. The optical cavity provides two major advantages over traditional VMS: greatly increased path length (about an order of magnitude greater than any previous VMS experiments, even with a cavity finesse of only 300) and the ability to observe a sub-Doppler Lamb dip for each spectral line (due to the high intracavity laser power and the perfectly overlapped counterpropagating beams induced by the optical cavity).

Although CEVMS showed much promise, its sensitivity was ultimately limited by noise in the laser-cavity lock, particularly noise that was induced by the high voltage AC plasma discharge. In the current work, the sensitivity limitations of CEVMS have been greatly improved by combining the technique with Noise Immune Cavity Enhanced Optical Heterodyne Molecular Spectroscopy (NICE-OHMS).

1.2. NICE-OHMS

NICE-OHMS is a technique that was first developed in the late 1990s [4], and has since been used with great success by several groups to observe spectra of many different neutral molecules with sensitivity unprecedented by other direct absorption spectroscopic techniques [5].

The principle of NICE-OHMS is that while the laser carrier frequency is locked to an optical cavity mode, a set of FM sidebands are added to the laser, spaced at an integer multiple of the cavity free spectral range (FSR). Thus the carrier (laser center frequency) and both sidebands get coupled into, and out of, the cavity simultaneously. The transmitted beam is detected with a fast photodiode and demodulated at the heterodyne modulation frequency.

Because the two sidebands have the same intensity when no absorbers are present within the cavity and are 180° out of phase with one another, the positive and negative RF beat signals created by the sideband frequencies beating against the carrier frequency cancel each other out, causing NICE-OHMS to be a zero-background technique. When the frequency modulated laser is coupled through the optical cavity and the sideband spacing is set to be exactly equal to the cavity FSR, any noise in the laser-cavity lock is the same for the carrier and both sidebands, so the demodulated signal is unaffected. Thus, NICE-OHMS allows for the path length enhancement of an optical cavity, a factor of $(2 \cdot Finesse/\pi)$, while not introducing any additional noise in the system beyond that of ordinary single-pass heterodyne spectroscopy.

An absorption signal is observed when one of the RF sidebands is absorbed more than the other, causing an imbalance in the two heterodyne beats, so they no longer add to zero. For any absorption, there is a corresponding dispersion, related by the Kramers-Kronig relations [6]. With heterodyne detection, it is possible to observe this dispersion signal, because a phase shift

#151471 - $15.00 USD Received 28 Jul 2011; revised 10 Oct 2011; accepted 17 Oct 2011; published 18 Nov 2011

in the carrier frequency or either of the sideband frequencies also creates an imbalance in the beat signals, leading to a net signal. The net signal obtained from a phase shift of one of the laser frequencies is 90° out of phase with that obtained from absorption of one of the sidebands, so through phase-sensitive detection, it is possible to observe absorption and dispersion independently of one another.

2. Experimental

The experimental setup is shown in Fig. 1. It is similar to that previously used for cavity-enhanced velocity modulation experiments [2, 3], with the addition of a second electro optic modulator (EOM) and a high speed photodiode for heterodyne detection.

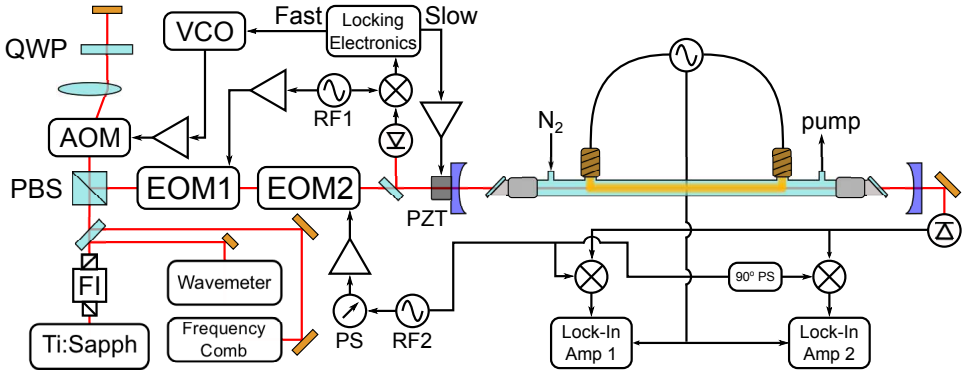

Fig. 1. Experimental Layout. FI: Faraday isolator; PBS: polarizing beamsplitter; AOM: acousto optic modulator; QWP: quarter wave plate; VCO: voltage controlled oscillator; EOM: electro optic modulator; PZT: piezo electric transducer; RF: radio frequency generator; PS: phase shifter.

The laser is double-passed through an acousto optic modulator that is resonant at 85 MHz, which red-shifts the laser frequency by 170 MHz and makes the pointing of the beam immune to changes in the acousto optic modulator (AOM) drive frequency [8].

The laser is then passed through two electro optic modulators, which add two sets of RF sidebands to the laser frequency. The first EOM, which is non-resonant, adds 30 MHz sidebands with a small modulation index ($\beta \sim 0.01$). These sidebands are detected in the back-reflected signal off of the cavity, and are demodulated with an RF mixer to generate a Pound-Drever-Hall [9] error signal. That error signal is then processed with analog electronics, and split off into two components; slow corrections (up to 100 Hz) are sent to the cavity piezo, while faster corrections (up to 60 kHz) are sent to the voltage controlled oscillator (VCO) that drives the acousto optic modulator AOM.

The second EOM, which is resonant, adds sidebands spaced at an integer multiple of the FSR of the optical cavity. The light transmitted through the cavity is detected with a fast photodiode. The AC portion of the detector signal is sent through an RF amplifier, then a power splitter that sends the signal to two mixers. The mixers are referenced to the sideband RF signal, but are set to be 90° out of phase with one another through a phase delay induced by a difference in cable lengths between the reference signal and the local oscillator (LO) input of the mixers. The overall detection phase is adjusted using an RF phase shifter in the line between the RF generator and the amplifier that drives the heterodyne EOM.

Two different experimental setups were used to observe several lines in the $v = 1 \leftarrow 0$ band of the Meinel system ($A^2\Pi_u - X^2\Sigma_g^+$) of N_2^+. One setup used a 1 GHz resonant EOM to space the

#151471 - $15.00 USD Received 28 Jul 2011; revised 10 Oct 2011; accepted 17 Oct 2011; published 18 Nov 2011

heterodyne sidebands at 9 cavity FSRs for observation of Doppler profiles and demonstration of ion-neutral discrimination. The other setup used a 113 MHz resonant EOM to space the sidebands at 1 cavity FSR for sub-Doppler studies of the observed Lamb dips.

The optical cavity used in both setups had a finesse of 300, which gave a cavity linewidth of 450 kHz. Throughout the course of a scan, the cavity length would change by 12 μm as the piezo was scanned, causing the FSR to change by approximately 1 kHz. To avoid increased noise near the end of the piezo travel, a feed-forward loop was implemented, in which the piezo voltage was scaled down, inverted, and sent to the DC FM input of the RF driver so the sideband spacing would track with the cavity FSR as the cavity length was scanned.

3. Results & discussion

3.1. Sub-Doppler lineshape analysis

Each laser frequency present in the cavity can act as a pump and/or a probe for sub-Doppler spectroscopy. For example, the carrier can act as a pump while a sideband acts as a probe, producing a Lamb dip spaced halfway between the two frequencies. Thus, Lamb dips are observed spaced at half the sideband spacing. For significant modulation depth ($\beta \sim 1$), where maximum heterodyne signal intensity is obtained, second-order sidebands also add small contributions to the outer edges of the signals. The overall sub-Doppler lineshape function is given by

$$\begin{aligned}\chi(\nu_d) = \{&A_1[\chi_a(\nu_d - \frac{\nu_{fm}}{2}) - \chi_a(\nu_d + \frac{\nu_{fm}}{2})] + A_2[\chi_a(\nu_d - \nu_{fm}) - \chi_a(\nu_d + \nu_{fm})] \\ &+ A_3[\chi_a(\nu_d - \frac{3\nu_{fm}}{2}) - \chi_a(\nu_d + \frac{3\nu_{fm}}{2})]\} \sin\theta_{fm} \\ &+ \{A_0[\chi_d(\nu_d)] + A_1[\chi_d(\nu_d - \frac{\nu_{fm}}{2}) + \chi_d(\nu_d + \frac{\nu_{fm}}{2})] \\ &+ A_2[\chi_d(\nu_d - \nu_{fm}) + \chi_d(\nu_d + \nu_{fm})]\} + A_3[\chi_d(\nu_d - \frac{3\nu_{fm}}{2}) + \chi_d(\nu_d + \frac{3\nu_{fm}}{2})]\} \cos\theta_{fm}\end{aligned} \tag{1}$$

where $\nu_d = \nu - \nu_0$ is the detuning of the laser center frequency, ν, from the transition center frequency, ν_0. ν_{fm} is the heterodyne modulation frequency and θ_{fm} is the heterodyne detection phase. $A_{0,1,2,3}$ are amplitudes related to the overall laser power and the modulation depth. In this work, these amplitudes are used as fit parameters with the constraint $A_i > A_{i+1}$.

χ_a and χ_d are general lineshape functions for absorption and dispersion profiles, respectively. In this work, the Lamb dips appear to be Gaussian, so χ_a is the general peak-normalized Gaussian lineshape, while χ_d is derived from χ_a transformed by the Kramers-Kronig relations [6]. The lineshape functions are given by [7]

$$\chi_a(\nu) = e^{-4\gamma^2} \qquad \text{and} \qquad \chi_d(\nu) = \frac{2}{\sqrt{\pi}} e^{-\gamma^2} \int_0^\gamma e^{\gamma'^2} d\gamma' \tag{2}$$

where w is the Gaussian full width at half maximum (FWHM), ν_0 is the line center, and $\gamma = 2(\ln 2)^{1/2}(\nu - \nu_0)/w$.

The combination of concentration and velocity modulation of N_2^+ causes the observed Doppler profile to be much different from those seen in other NICE-OHMS setups that observe neutral molecules. In this work, no attempt was made at fitting the overall Doppler broadened lineshapes; the Doppler broadened profile was approximated by a third order polynomial near the line center that was used as a baseline for sub-Doppler fitting.

3.2. 1 GHz sideband spacing

The 1 GHz system, with sidebands spaced at 9 FSRs, was used for Doppler-broadened scans. Figure 2 shows a typical scan with this system, collected with a 300 ms lock-in time constant,

#151471 - $15.00 USD Received 28 Jul 2011; revised 10 Oct 2011; accepted 17 Oct 2011; published 18 Nov 2011

100 ms delay between points, and approximately 10 MHz step size. With this setup, only a single mixer and lock-in amplifier were used, and the RF phase was set to be nearly pure dispersion, as evidenced by the presence of a strong central Lamb dip, which is expected to be absent from the pure absorption signal.

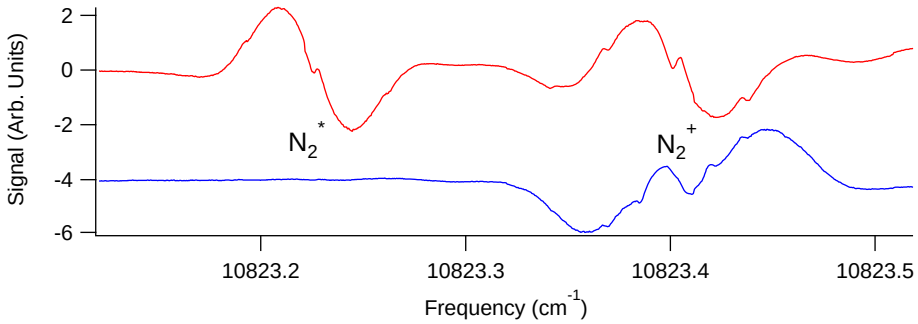

Fig. 2. A scan with 1 GHz sideband spacing, demonstrating discrimination between N_2^+ and N_2^*. At the left is an unassigned transition of electronically excited neutral N_2. At the right is an unresolved blend of two N_2^+ lines, $Q_{12}(6)$ and $Q_{11}(14)$. The top and bottom traces are the X and Y channels of the lock-in amplifier, rotated in post-processing by 64°.

During data collection, the lock-in amplifier phase was set to zero. After collection of the data, computer software was used to rotate the phase of the signal with respect to the plasma frequency in order to minimize the amount of N_2^* signal present in the Y channel. Note that just the concentration of N_2^* is modulated in the plasma, so its Doppler-broadened profile is similar to other NICE-OHMS lineshapes that are typically observed for neutral molecules [10]. With N_2^+, however, both the velocity and concentration are being modulated simultaneously, which leads to a more complex lineshape that cannot be isolated into a single phase.

3.3. 113 MHz sideband spacing

For spectroscopy with sidebands spaced at a single cavity FSR, both RF mixers were used, and the lengths of cables going to the LO inputs of the two mixers were made such that the relative phases were 90° apart. The overall phase of the system was adjusted to optimize the isolation of absorption and dispersion signals using an electronic phase shifter on the input to the amplifier that drives EOM2.

A typical scan with the 113 MHz system, calibrated with an optical frequency comb, as described in [3], is shown in Fig. 3. A single scan produces four orthogonal signals: absorption and dispersion, each with X and Y components. Absorption and dispersion signals are first separated using the 90° phase difference in the RF mixer references, then each of these is split into two components separated by 90° relative to the plasma frequency by mixers within the lock-in amplifiers. Fits were performed on the Lamb dips of the comb-calibrated scans using Eq. (1), along with a cubic sloped baseline to approximate the Doppler profile near the line center. Note that the residuals show that the actual lineshape is more complex than that given in Eq. (1) due to the combination of concentration modulation and velocity modulation occurring in the plasma. A more thorough lineshape analysis will be the subject of future studies.

Based on fits of several scans in alternating directions, calibrated with an optical frequency comb, the measured line center frequency was found to have a standard deviation of approximately 2 MHz. Because of the delayed response of the lock-in amplifiers used for demodulation, the determined line centers tend to be shifted in the direction of the scanning. By pairing

#151471 - $15.00 USD Received 28 Jul 2011; revised 10 Oct 2011; accepted 17 Oct 2011; published 18 Nov 2011

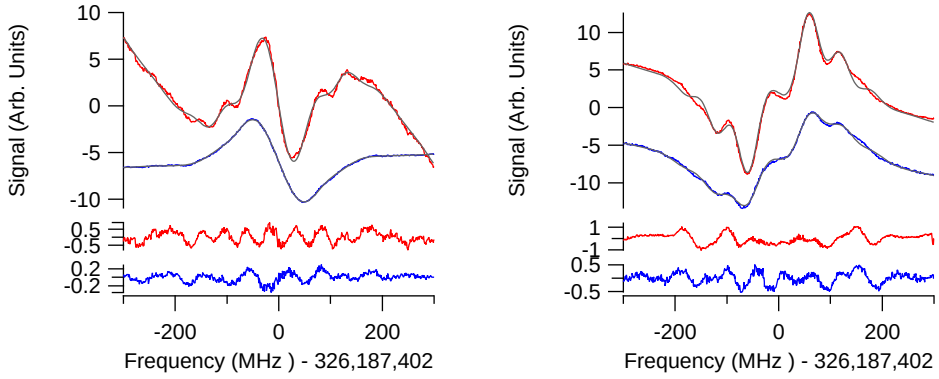

Fig. 3. Dispersion (left) and absorption (right) Lamb dips of the $Q_{22}(13)$ line of N_2^+ observed in the 113 MHz configuration, calibrated with an optical frequency comb. Top, red: Y channel outputs of lock-ins. Bottom, blue: X channel outputs of lock-ins, offset vertically for clarity. Residuals are shown at the bottom.

and averaging pairs of scans in opposite directions, the measurement standard deviation can be reduced to ∼300 kHz. It was found that the line center frequencies determined previously in Ref [3] were all too high by 20 MHz due to an ambiguity in the determination of the sign of the comb carrier-envelope offset.

The pressure broadening of ∼8 MHz/Torr of the observed Lamb dips observed in Ref [3] and in the current work is consistent with the expected broadening given by the total collision cross section given by Eq. (5.69) of Ref [11] integrated over the Maxwell-Boltzmann distribution for the estimated plasma temperature (∼600 K), but the extrapolated ∼32 MHz linewidth at zero pressure is still not fully understood.

4. Conclusions & future work

The technique of cavity enhanced velocity modulation spectroscopy has been further improved by the addition of heterodyne detection to minimize the noise induced by the laser-cavity lock. This modification has improved upon the achievable sensitivity of CEVMS by nearly two orders of magnitude while retaining ion-neutral discrimination. Combined with an optical frequency comb, line centers can be determined to within 300 kHz.

Further improvement to this technique can be realized by moving to a higher finesse cavity to increase both the effective path length and the intracavity optical power. Moving to a higher finesse cavity would cause this technique to be more sensitive to mismatches in the cavity FSR and RF sideband frequency due to the narrower cavity resonances. This effect could be compensated for by actively locking the RF sideband frequency to the cavity FSR using the DeVoe-Brewer [12] method, rather than the less precise feed-forward loop that was used in this work. This technique could also be extended to mid-infrared wavelengths by using a high power optical parametric oscillator (OPO) to observe a much greater variety of molecular ions.

Acknowledgments

This work has been supported by an NSF CAREER award (CHE 04-49592), an Air Force Young Investigator award (FA9550-07-1-0128), the NASA Laboratory Astrophysics program (NNX08AN82G), a David and Lucile Packard Fellowship, and the University of Illinois. Michael Porambo has been supported by a Robert C. and Carolyn J. Springborn Fellowship.

#151471 - $15.00 USD Received 28 Jul 2011; revised 10 Oct 2011; accepted 17 Oct 2011; published 18 Nov 2011